

OPEN ACCESS

Phenolic Resin as an Inexpensive High Performance Binder for Li-Ion Battery Alloy Negative Electrodes

To cite this article: T. D. Hatchard *et al* 2016 *J. Electrochem. Soc.* **163** A2035

View the [article online](#) for updates and enhancements.



ECS Membership = Connection

ECS membership connects you to the electrochemical community:

- Facilitate your research and discovery through ECS meetings which convene scientists from around the world;
- Access professional support through your lifetime career;
- Open up mentorship opportunities across the stages of your career;
- Build relationships that nurture partnership, teamwork—and success!

Join ECS!

Visit electrochem.org/join





Phenolic Resin as an Inexpensive High Performance Binder for Li-Ion Battery Alloy Negative Electrodes

T. D. Hatchard,* P. Bissonnette, and M. N. Obrovac*^z

Department of Chemistry, Dalhousie University, Halifax, N. S. B3H 4R2, Canada

Phenolic resin was evaluated as a binder material for Li-ion battery negative electrodes containing Si-based alloys. Phenolic resin was found to have a large first lithiation capacity of about 1200 mAh/g, which is suspected to result from the full reduction of the phenolic resin to form a hydrogen containing carbon. The decomposition products formed during the first lithiation have a reversible capacity of about 400 mAh/g and have excellent properties as a binder for alloy-based negative electrodes. The excellent performance of the phenolic resin combined with its low cost make it very attractive for use as a binder in alloy containing negative electrodes for Li-ion batteries. Furthermore the use of binders that decompose during lithiation represents a new concept in the design of high performance binder materials.

© The Author(s) 2016. Published by ECS. This is an open access article distributed under the terms of the Creative Commons Attribution Non-Commercial No Derivatives 4.0 License (CC BY-NC-ND, <http://creativecommons.org/licenses/by-nc-nd/4.0/>), which permits non-commercial reuse, distribution, and reproduction in any medium, provided the original work is not changed in any way and is properly cited. For permission for commercial reuse, please email: oa@electrochem.org. [DOI: 10.1149/2.1121609jes] All rights reserved.

Manuscript submitted April 7, 2016; revised manuscript received July 12, 2016. Published July 22, 2016.

As the drive to increase the capacity and energy density of Li-ion batteries continues, much work is focused on finding better electrode materials. Much attention has been given to Si and Si-based alloys because of the obvious benefits of the high theoretical capacity of Si. However, this high capacity comes with a price: the large volume changes during charge/discharge cycling that lead to electrode failure.¹ To deal with this problem, many researchers are developing advanced binders. Such binders do not limit the volume expansion experienced during lithiation, but maintain structural integrity and electrical connection to the alloy particles during cycling.²⁻⁴ It has been shown that good binders for alloy materials provide good adhesion to the active materials and to the current collector, and also provide complete coverage of the alloy particle surfaces.² It is suspected that by completely covering the surface of the alloy particles, binders can form an “artificial SEI” layer to reduce electrolyte decomposition reactions.² Examples of binders that exemplify these properties and result in good cycling performance in alloy negative electrodes include poly(carboxylic acids) and their alkali metal salts, including carboxymethyl cellulose (CMC),⁵⁻¹⁰ poly(acrylic acid) (PAA)^{4,11-13} and alginate.¹⁴ Other studies have shown that conductive polymers can also be used as excellent binders for alloy negative electrodes.^{15,16}

Aromatic polyimides (aro-PI) have been shown to be an excellent binder for alloy negative electrodes.^{17,18} Recently, we have shown that aro-PI has a very large first lithiation capacity of 1943 mAh/g, corresponding to a 34 electron reduction process.¹⁹ This reduction capacity is consistent with the charge required to fully decompose the aro-PI to a hydrogen containing carbon. The resulting decomposition products also had similar electrochemical properties as hydrogen containing carbon, with a reversible capacity of 874 mAh/g, leading to added electrode capacity. Alloy negative electrodes using aro-PI binder had excellent cycling performance. It was suspected that if a hydrogen containing carbon was formed during the first lithiation, it could provide a conductive framework, enabling excellent charge/discharge cycling. Indeed, it has been recently shown that thermally carbonized binders can have excellent performance in alloy negative electrode coatings.²⁰

However, the reduction reaction of aro-PI also results in a large first cycle irreversible capacity of the electrode. Conductive polymers also exhibit this high irreversible capacity.¹⁹ We suspect that they are also undergoing carbonization during their first lithiation. If carbonization of the binder is key to good cycling properties the utility of using expensive polyimide-based or conductive binders is questionable, when other more inexpensive polymers may exist that undergo reduction during lithiation to produce conductive species.

In Reference 19 we speculated that all electrochemically active aromatic binders might carbonize and have good cycling properties in alloy electrode coatings. If so, this would present a new concept for the design of good binders for alloy materials. Since cost is important to industrial implementation of binder materials, we chose to verify this concept using the most inexpensive polymers that we could think of that would likely be electrochemically active and undergo reduction during lithiation, namely aromatic phenolic resins. An example of a basic phenolic resin structure is shown in Figure 1. Because of their extremely low cost, phenolic resins are widely used as binders in applications such as sandpaper, roofing materials and wood adhesives. In this letter, we will show that phenolic resin is an exemplary binder for alloy negative electrodes.

Experimental

Electrode preparation.—Electrode coatings were made by mixing active material, binder and carbon black (Super C65, TimCal) in N-methyl-2-pyrrolidone (NMP, Sigma Aldrich, anhydrous 99.5%) in specific ratios. The active materials for alloy/graphite blended coatings were a Si-based alloy from 3M Company known as V6 (3M L-20772 V6 Si alloy, 3M Co., St. Paul, MN) and SFG6L graphite (TimCal). The electrode formulation was based on an optimized alloy/graphite ratio as described in Reference 3, and consisted of 60% V6, 28% SFG6L, 2% Super C and 10% binder (by weight). For graphite only coatings, a 90/5/5 by weight formulation of SFG6L/Super C/binder was used. The binders used were aromatic polyimide (20% solution in N-methyl-2-pyrrolidone (NMPP, HD MicroSystems) and phenolic resin (3M RPR1, resole phenol-formaldehyde resin, having phenol to formaldehyde ratio of 1.5–2.1/1, catalyzed with 2.5 percent potassium hydroxide, ~75% solution in water, 3M Co.). Polyvinylidene difluoride (PVDF, average MW ~534,000 by GPC, powder, Sigma-Aldrich)

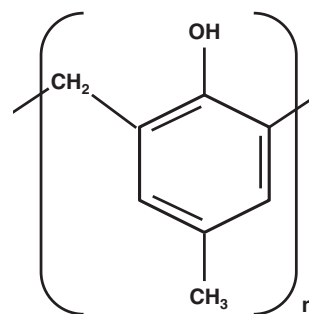


Figure 1. Example of the structure of a basic phenolic resin.

*Electrochemical Society Member.

^zE-mail: mnobrovac@dal.ca

was also used in some graphite-only coatings. The phenolic resin was diluted with NMP (Sigma Aldrich, anhydrous 99.5%) to make a 20% by weight solution before using to make electrode slurries. Slurries were mixed for one hour in a Retsch PM200 planetary mill at 100 rpm with four $\frac{1}{2}$ " tungsten carbide balls and then spread onto copper foil with a 0.004" doctor blade. Coatings were dried in air at 120°C for one hour, and then cured under flowing Ar by heating to 300°C at a rate of 5°C/min and then held at 300°C for 3 hours. Coatings using PVDF binder were not subjected to heating after being dried at 120°C. The electrodes were then taken into an Ar filled glove box for cell assembly without air exposure. Active material loadings ranged from 1.5 to 2.1 mAh/cm² or about 2–3 mg/cm². TiN (99.7% Alfa Aesar) /phenolic resin electrodes were prepared in a 83/17 v/v ratio of TiN/phenolic resin (95.6/4.4 w/w) by the same method as described in Reference 19.

Coin cell preparation.—Circular electrodes with an area of 1.9 cm² were punched from the electrode coatings. Coin cells were assembled in an argon-filled glove box using lithium metal foil (99.9%, 0.38 mm thick, Aldrich) as common counter and reference electrode with two layers of Celgard 2301 as the separator. The electrolyte was 1 M LiPF₆ in a solution of ethylene carbonate, diethyl carbonate and monofluoroethylene carbonate (EC/DEC/FEC; 3:6:1 by volume, all battery grade from BASF). Alloy coin cells were cycled on a Maccor Series 4000 Automated Cycler. For the first cycle the voltage limits were from 0.005–1.5 V and the cell was discharged (lithiation of the alloy) at a rate of C/10 to 0.005 V, then held at constant voltage until the current dropped to C/20 rate. The cell was then charged (delithiation of the alloy) at a C/10 rate to 1.5 V. Here C-rate was calculated based on an alloy capacity of 900 mAh/g and a graphite capacity of 370 mAh/g. During the second and subsequent cycles the cell was discharged to 0.005 V at a C/4 rate and held at this voltage until the current dropped to C/20, and then the cell was charged to 0.9 V. These cycling conditions were chosen to simulate the cycling conditions of negative electrodes in commercial Li-ion cells using a “CCCV” protocol, as described in Reference 21. TiN/phenolic resin coatings were cycled between 0.005 V and 2 V versus Li/Li⁺ at a rate of C/10, where C-rate was calculated based on a reversible phenolic resin capacity of 400 mAh/g. After each discharge the cells were held at 0.005 V until the current dropped to a C/20 rate before starting the next charge cycle. This was again done to simulate the CCCV cycling protocol typically used in commercial cells.

Results and Discussion

TiN/phenolic resin coatings were used to measure the electrochemistry of phenolic resin (PR) in Li cells. In such coatings, the PR is in the same environment (coated in a thin layer on conductive particles) as it would be in a composite electrode coating. Since the TiN is inactive, the electrochemical behavior of the coating can be attributed to the binder.¹⁹ Figures 2a–2c show the voltage curve, differential capacity, and cycling performance respectively, of a TiN/PR coating vs. Li. The voltage curve of PR shows a large lithiation capacity, a large irreversible capacity, followed by reversible cycling between 0 V and 2 V accompanied by large hysteresis. The voltage curve is similar to that observed for hydrogen containing carbons.²² Initial features in the differential capacity above 0.8 V are likely due to SEI formation and water reduction.²³ This is followed by a high capacity reduction reaction at low voltage, resulting in a total initial lithiation capacity of 862 mAh/g (standard deviation of first discharge capacity for a set of cells averaged 27 mAh/g). Although this TiN/PR coating gives insight with respect to the voltage curve and reversibility of PR, it does not accurately reflect its lithiation capacity, as will be discussed below.

Figure 3 shows a plot of the first lithiation capacity as a function of the PR volume percent in a number of TiN/PR coatings. As the PR content in the coating decreases, its initial lithiation capacity increases. We believe this behavior is due to the contribution to the first cycle capacity from the formation of the solid electrolyte interface (SEI) layer. For instance, there would be SEI capacity for a TiN coating even when

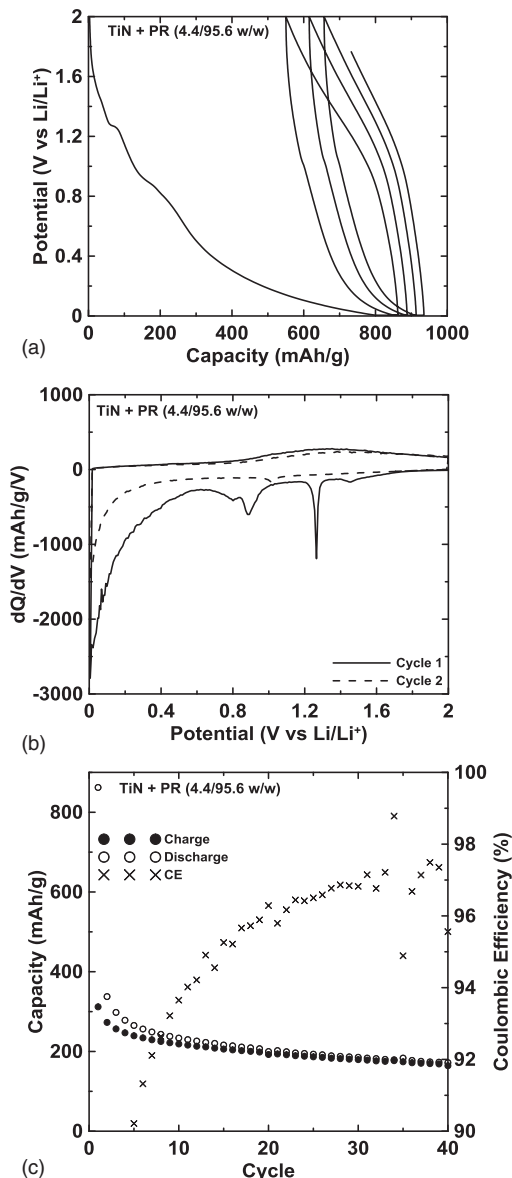


Figure 2. Plots of (a) voltage versus capacity, (b) differential capacity and (c) cycling performance of a TiN/phenolic resin electrode (95.6/4.4 w/w), in which the phenolic resin is the only electrochemically active component.

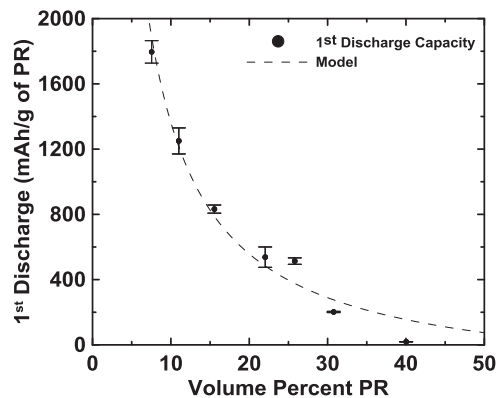


Figure 3. First lithiation capacity of PR versus the volume percent PR in TiN/PR coatings. The dashed line is a fit to the data based on the capacity having an inverse relationship to the PR volume percent.

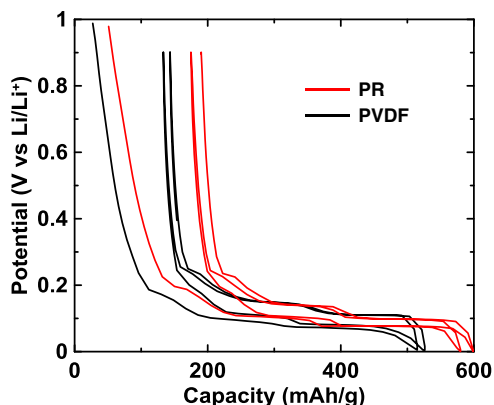


Figure 4. Voltage curves of graphite electrodes using PR and PVDF binders.

PR is not present. Because of this, the first lithiation PR specific capacity would approach infinity as the PR content approached zero. This effect should result in the first lithiation PR specific capacity in these coatings being inversely proportional to the PR content at low PR contents. Indeed, this inverse relationship does seem to exist as is illustrated by the fitted line shown in the figure. However, in addition to this inverse relationship, there is likely a reduction in capacity as the film becomes thicker and some of the PR becomes inaccessible for reaction with lithium, which we have observed previously for PI binders.¹⁹ At contents above 30 volume percent, the PR becomes inactive. The same behavior was observed for PI binders and occurs when the TiN in the coating no longer makes a percolating path to the electrode surface, thus impeding any electrochemical reactions.¹⁹ Therefore, as observed for aro-PI, coatings with PR binder will become electrochemically inactive when the PR loading becomes too high. The effects observed here make the determination of the exact PR capacity difficult.

To quantitatively measure the PR capacity, and to gauge its impact on electrode capacity when used as a binder, the electrochemical behavior of a graphite coating using PR binder was compared to that with a PVDF binder. Figure 4 shows the voltage curve of these electrodes. The coating with PR binder has a much larger first lithiation capacity (555 ± 20 mAh/g for PR, 467 ± 14 mAh/g for PVDF) and irreversible capacity ($41.9 \pm 0.9\%$ for PR, $32.1 \pm 0.3\%$ for PVDF). It is interesting that the PR coating also has much smaller voltage polarization. This would be expected if the PR is becoming reduced during the first lithiation to form a conductive carbon. Both of these electrodes cycle with little fade. Since PVDF is expected to have no electrochemical activity, and assuming the capacity due to SEI formation in both electrodes is similar, the difference in the capacity of these two electrodes should correspond to the PR capacity. Figure 5 shows the PR capacity as calculated from the difference between the graphite/PR electrode and graphite/PVDF electrode capacities.

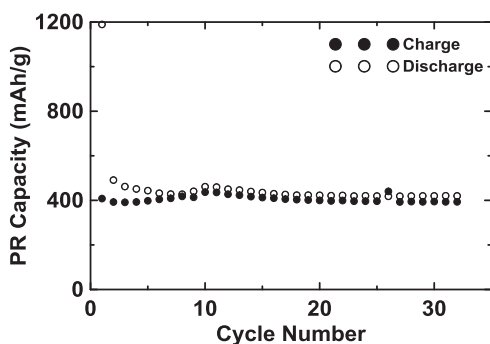


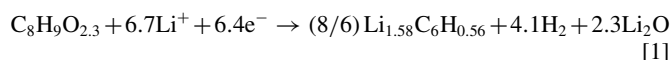
Figure 5. Capacity vs. cycle number of phenolic resin calculated as the difference between the capacities of the graphite coatings with PR and PVDF binders shown in Figure 4.

Table I. Electrochemical properties of phenolic resin and aromatic polyimide binders. Aro-PI capacities are from Reference 19.

Binder	First Lithiation Capacity (mAh/g)	Reversible Capacity (mAh/g)
PR	1200	400
aro-PI	1943	874

The initial lithiation capacity of PR is about 1200 mAh/g and has a reversible capacity of about 400 mAh/g with little fade over the 30 cycles shown. Table I lists the reversible and irreversible capacity of PR and PI binders for comparison.

Considering a nominal molecular formula of the cured PR to be $C_8H_9O_{2.3}$, the 1200 mAh/g reduction of PR corresponds to a 6.4 electron reduction per formula unit. This is large a capacity for such a small formula unit and suggests that the PR is being nearly fully reduced. Considering the voltage curve of PR, shown in Figure 2a, is similar to a hydrogen containing carbon, a plausible reduction reaction may be given as:



Here the total capacity from the hydrogen containing carbon was chosen to be 2.1Li, in order to correspond to the 400 mAh/g observed reversible capacity of PR. The hydrogen containing carbon lithiation level is according to the model of Zheng and Dahn, where carbon can reversibly form LiC_6 and each hydrogen results in the uptake of an additional lithium.²² Additional lithium is expected to react with the oxygen in the PR to produce Li_2O . Reaction 1 corresponds to a 6.7 electron reduction and a 2.1 electron reversible capacity, which is almost exactly what is observed. Therefore the first lithiation and reversible capacity of PR can be well described as an initial reduction to a hydrogen containing carbon, followed by reversible cycling of the carbon product. We have suggested that a similar reaction occurs for aro-PI binders.¹⁹

The performance of PR binder was also evaluated in electrodes having a 60/28 weight ratio of 3M V6 Si alloy and graphite. The mechanical properties of such electrodes were excellent and similar to electrodes using LiPAA binder. The electrode could be bent over 90° without delamination, and there was no evidence of swelling when soaked in electrolyte solution for 24 hours. The porosity of the un-calendared electrode after heating to $300^\circ C$ was measured to be $\sim 62\%$, which is comparable to the LiPAA electrode in Reference 3. The percent volume expansion of the electrode with PR binder was determined by comparing as coated thickness to the thickness of a fully discharged electrode, and was found to be $57 \pm 12\%$, in accordance with the 53% volume expansion expected based on an alloy expansion of 109% and a constant porosity of 62 volume percent.³

Figure 6 shows the voltage versus capacity curves of V6 alloy/graphite electrodes made with LiPAA (lithium salt of polyacrylic

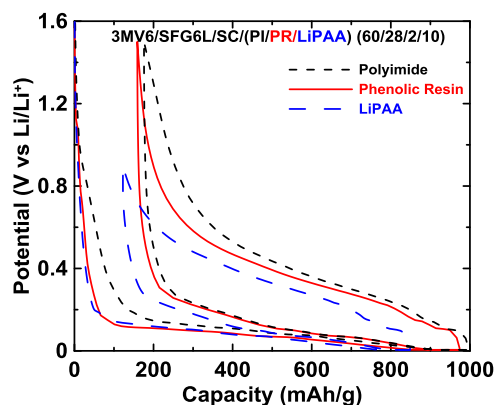


Figure 6. Voltage curves of 3M V6 alloy/graphite composite electrodes using aro-PI, LiPAA, and PR binders.

Table II. Observed and predicted capacities of V6/graphite coatings with different binders. The LiPAA coating capacities are from Reference 9. The capacities of the coatings with PR and aro-PI binders were calculated by adding the binder capacities listed in Table I, to the capacities of the LiPAA coating.

Binder	First Lithiation Capacity (mAh/g)		Irreversible Capacity (mAh/g)		Reversible Capacity (mAh/g)	
	Observed	Predicted	Observed	Predicted	Observed	Predicted
LiPAA	848	-	122	-	726	-
PR	974	934	190	202	784	766
aro-PI	997	1042	213	229	783	813

acid, as described in Reference 10), aro-PI binder or PR binder. Here, all specific capacities of V6 alloy/graphite electrodes are given per total electrode mass. LiPAA is not an electrochemically active binder and does not contribute to the reversible or irreversible capacity.¹⁹ As expected, the electrode with PR binder has a greater first lithiation and reversible capacity than the coating with LiPAA binder, since the electrochemically active PR binder contributes to the coating's capacity. Similarly, aro-PI binder has a higher first lithiation and reversible capacity than PR, and, as expected, the coating with aro-PI binder has

the highest first lithiation and reversible capacity of all three coatings. The additional capacity imparted to the coatings by the binders can be predicted using the measured binder capacities from TiN/binder coatings. This is demonstrated in Table II, where the PR and aro-PI capacities listed in Table I were used to calculate the additional coating capacity imparted by the binder. These additional capacities were then added to the LiPAA coating capacity to predict the capacities of the V6 alloy/graphite electrodes with aro-PI and PR binders. The predicted capacities are within 10% of the observed values. This demonstrates the utility of measuring the capacity of electrochemically active binders, as they can make a significant contribution to the total electrode capacity.

Figures 7a–7c shows the capacity and the coulombic efficiency (delithiation capacity/previous lithiation capacity) versus cycle number for V6 alloy/graphite electrodes made with LiPAA, aro-PI or PR binders, respectively. All electrodes have good cycling performance and similar coulombic efficiencies. LiPAA is an example of a non-active binder with low first cycle capacity. As we suggest here, aro-PI and PR are both examples of binders that form conductive networks of active hydrogen containing carbons. Both binders perform very well, with little to no capacity fade during the first 80 cycles. There is also little evidence for impedance growth, with the voltage polarization between charge and discharge increasing by 0.02 V over this cycle range (compared to ~0.110 V for similar electrodes using PVDF binder), which could be attributed to impedance growth on the Li counter/reference electrode in the half cells used for testing. However, PR binder is expected to be much less expensive than aro-PI. Further experiments in full lithium ion cells are needed to compare the benefits of these two types of approaches to high performance binders for alloy negative electrodes.

Conclusions

PR was found to be an electrochemically active binder with 1200 mAh/g initial lithiation capacity and 400 mAh/g reversible capacity. This capacity is consistent with a nearly full reduction of PR to a hydrogen containing carbon. After the first lithiation, the hydrogen containing carbon thus formed can cycle reversibly to contribute capacity to the electrode. PR was employed as the binder material in a composite anode consisting of a Si-based alloy and graphite. It was found that the cycling performance of PR binder is similar to that of aro-PI or LiPAA binders. In addition, PR is likely much less expensive than aro-PI. This demonstrates a second example of a high performance binder obtained from an electrochemically active polymer that decomposes during lithiation. We suspect this might be a general property of aromatic polymers. If so, this presents a new concept for the design of high performance binders for alloy electrode coatings and it is likely that many more good binders based on inexpensive electrochemically active polymers exist. More in depth studies on phenolic resins and other inexpensive electrochemically active polymers for use as binders in alloy electrodes are needed.

References

- M. N. Obrovac, L. Christensen, Dinh Ba Le, and J. R. Dahn, *J. Electrochem. Soc.*, **154**, A849 (2007).
- M. N. Obrovac and V. L. Chevrier, *Chemical Reviews*, **114**(23), 11444 (2014).

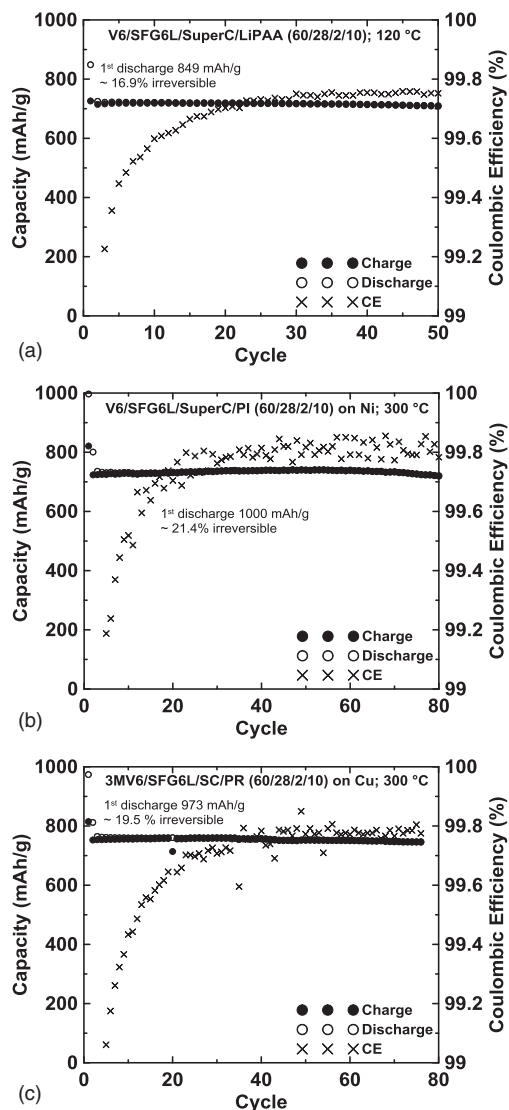


Figure 7. Capacity versus cycle number and coulombic efficiency versus cycle number for 3M V6 alloy/graphite composite electrodes using (a) LiPAA (from Reference 3), (b) aro-PI, and (c) PR binders.

3. Z. Du, R. A. Dunlap, and M. N. Obrovac, *Journal of The Electrochemical Society*, **161**(10), A1698 (2014).
4. S. Komaba, K. Shimomura, N. Yabuuchi, T. Ozeki, H. Yui, and K. Konno, *J. Phys. Chem. C*, **115**, 13487 (2011).
5. J.-S. Bridel, T. Azais, M. Morcrette, J.-M. Tarascon, and D. Larcher, *Chem. Mater.*, **22**, 1229 (2010).
6. W.-R. Liu, M.-H. Yang, H. Wu, S. M. Chiao, and N.-L. Wu, *Electrochem. Solid-State Lett.*, **8**, A100 (2005).
7. B. Lestriez, S. Bahri, I. Sandu, L. Roue, and D. Guyomard, *Electrochem. Commun.*, **9**, 2801 (2007).
8. N. S. Hochgatterer, M. R. Schweiger, S. Koller, P. R. Raimann, T. Woöhrle, C. Wurm, and M. Winter, *Electrochem. Solid-State Lett.*, **11**, A76 (2008).
9. J.-S. Bridel, T. Azais, M. Morcrette, J.-M. Tarascon, and D. Larcher, *J. Electrochem. Soc.*, **158**, A750 (2011).
10. M. Cerbelaud, B. Lestriez, D. Guyomard, A. Videcoq, and R. Ferrando, *Langmuir*, **28**, 10713 (2012).
11. S. Komaba, N. Yabuuchi, T. Ozeki, Z. Han, K. Shimomura, H. Yui, Y. Katayama, and T. Miura, *J. Phys. Chem. C*, **116**, 1380 (2012).
12. J. Li, D.-B. Le, P. Ferguson, and J. R. Dahn, *Electrochim. Acta*, **55**, 2991 (2010).
13. A. Magasinski, B. Zdyrko, I. Kovalenko, B. Hertzberg, R. Burtovyy, C. F. Huebner, T. F. Fuller, I. Luzinov, and G. Yushin, *ACS Appl. Mater. Interfaces*, **2**, 3004 (2010).
14. I. Kovalenko, B. Zdyrko, A. Magasinski, B. Hertzberg, Z. Milicev, R. Burtovyy, I. Luzinov, and G. Yushin, *Science*, **334**, 75 (2011).
15. G. Liu, S. Xun, N. Vukmirovic, X. Song, P. Olalde-Velasco, H. Zheng and V. S. Battaglia, L. Wang and W. Yang, *Adv. Mater.*, **23**, 4679 (2011).
16. S. Xun, X. Song, V. Battaglia, and G. Liu, *Journal of The Electrochemical Society*, **160**(6) A849 (2013).
17. A. Guerfi, P. Charest, M. Dontigny, J. Trottier, M. Lagacé, P. Hovington, A. Vijh, and K. Zaghbi, *Journal of Power Sources*, **196**(13), 5667 (2011).
18. Q. Yuan, F. Zhao, Y. Zhao, Z. Liang, and D. Yan, *Journal of Solid State Electrochemistry*, **18**(8), 2167 (2014).
19. B. N. Wilkes, Z. L. Brown, L. J. Krause, M. Triemert, and M. N. Obrovac, *Journal of The Electrochemical Society*, **163**(3), A364 (2016).
20. J. S. Kim, W. Choi, K. Y. Cho, D. Byun, J. Lim, and J. K. Lee, *Journal of Power Sources*, **244**, 521 (2013).
21. Vincent L. Chevrier, Li Liu, Dinh Ba Le, Jesse Lund, Biniam Molla, Karl Reimer, Larry J. Krause, Lowell D. Jensen, Egbert Figgemeier, and Kevin W. Eberman, *Journal of the Electrochemical Society*, **161**, A783 (2014).
22. T. Zheng, W. R. MacKinnon and J. R. Dahn, *Journal of The Electrochemical Society*, **143**(7), 2137 (1996).
23. D. Aurbach, M. Daroux, P. Faguy, and E. Yeager, *J. Electroanal. Chem.*, **297**, 225 (1991).